The origin and liver repopulating capacity of murine oval cells

Xin Wang*, Mark Foster*, Muhsen Al-Dhalimy*, Eric Lagasse†, Milton Finegold‡, and Markus Grompe*§¶

Departments of *Molecular and Medical Genetics and §Pediatrics, Oregon Health Sciences University, 3181 Southwest Sam Jackson Park Road, Portland, OR 97239; †Stem Cells Inc., Palo Alto, CA 94304; and ‡Department of Pathology, Texas Children's Hospital, Houston, TX 77030

The appearance of bipotential oval cells in chronic liver injury suggests the existence of hepatocyte progenitor/stem cells. To study the origin and properties of this cell population, oval cell proliferation was induced in adult mouse liver by 3,5-diethoxycarbonyl-1,4-dihydrocollidine (DDC) and a method for their isolation was developed. Transplantation into fumarylacetoacetate hydrolase (Fah) deficient mice was used to determine their capacity for liver repopulation. In competitive repopulation experiments, hepatic oval cells were at least as efficient as mature hepatocytes in repopulating the liver. In mice with chimeric livers, the oval cells were not derived from hepatocytes but from liver nonparenchymal cells. This finding supports a model in which intrahepatic progenitors differentiate into hepatocytes irreversibly. To determine whether oval cells originated from stem cells residing in the bone marrow, bone marrow transplanted wild-type mice were treated with DDC for 8 months and oval cells were then serially transferred into *Fah* mutants. The liver repopulating cells in these secondary transplant recipients lacked the genetic markers of the original bone marrow donor. We conclude that hepatic oval cells do not originate in bone marrow but in the liver itself, and that they have valuable properties for therapeutic liver repopulation.

In mammals, hepatic cells, especially hepatocytes can rapidly proliferate after acute liver injury to repair liver damage (1). Usually, undifferentiated liver progenitors do not take part in such acute liver regeneration. However, hepatocyte progenitors are still required in some chronic injury responses, especially when the ability of differentiated hepatocytes to divide is impaired (reviewed in refs. 2 and 3). The existence of endogenous stem cells inside mammalian liver was first suggested by the observation that treatment with carcinogens results in the emergence of oval cells in the portal region of the hepatic lobule (4–9). Oval cells are ≈10 μm in size, have a high nuclear/cytoplasmic ratio, and express markers of immature liver cells such as α-fetoprotein (AFP) (10, 11). In addition, oval cells express markers of both the biliary epithelium (CK19) and hepatocyte lineages (albumin). *In vitro*, these cells can be differentiated into both of these hepatic epithelial lineages under appropriate conditions.

Although the anatomical location of the oval cell proliferation suggests the existence of a hepatocyte progenitor in the Canal of Hering (12), the precise origin of oval cells remains uncertain. Most studies imply the existence of an undifferentiated oval cell precursor in this location that proliferates and gives rise to oval cells (13–16). In analogy to the hematopoietic system, oval cells would then represent a committed bipotential progenitor. Recent studies in both rat and human have suggested that oval cells could be derived from precursors in the bone marrow (17). Others, however, have postulated that oval cells may arise by dedifferentiation of hepatocytes, not from a nonparenchymal progenitor (18, 19). Rat hepatocytes can be cultured for extended periods and then differentiated into bile-duct epithelium *in vitro*, indicating the bipotentiality of differentiated hepatocytes (18, 20, 21). Similarly, it has been shown that the small basophilic foci induced by carcinogen treatment in the mouse were hepatocyte-derived, not progenitor-derived (19).

Oval cells and their intrahepatic progenitors have also been of interest in the field of liver cell transplantation and therapeutic liver repopulation (22, 23). Although oval cells have been used for cell transplantation (24, 25), no reports describing the use of oval cells for therapeutic liver repopulation have been reported.

Here we used treatment with 3,5-diethoxycarbonyl-1,4-dihydrocollidine (DDC) to induce oval cell (atypical duct cell) proliferation in mice (26). To address the origin of these oval cells in mouse liver regeneration and to test their potential in cell therapy, we performed transplantation experiments in the fumarylacetoacetate hydrolase (Fah) knockout mouse (27, 28).

Materials and Methods

Mouse Strains and Animal Husbandry. We used the *Fah*Δexon 5 mouse strain as transplantation recipient as described (27). Donor hepatocytes were from transgenic *Rosa*-26 mice, a gift from P. Soriano (29). All transplantations were performed with congenic mice on the $129S_4$ background. All *Fah* mutants were maintained on 2-(2-nitro-4-trifluoromethylbenzoyl)-1,3-cyclohexanedione (NTBC) in their drinking water as described (30, 31). Genotyping was carried out with a three-primer PCR on 200-ng tail-cut DNA as described (27). Animal care and experiments were all in accordance with the Guidelines of the Department of Animal Care at Oregon Health and Science University.

Oval Cell Harvest, Fractionation, and Sizing. Mice were treated with a DDC diet (0.1% wt/wt in Purina 5015 mouse chow) for 3–6 weeks. After mice were killed, both hepatocytes and liver nonparenchymal cells were harvested by a multiple-step digestion with proteases. First, the hepatocytes were collected by a two-step *in situ* perfusion with collagenase D (Roche Applied Science, 0.45 mg/ml) as described (28). Afterward, the remaining, undigested liver nonparenchymal tissue was collected and further digested in a medium containing both collagenase D (Roche Applied Science, 1 mg/ml) and pronase (Roche Applied Science, 1 mg/ml) combined with DNase I (DN-25, Sigma, 0.1 mg/ml) for 30–40 min at 37°C by using a stir bar. The digestion mix was filtered through a 70-μm nylon mesh to get a single cell suspension. After washing twice with DMEM (GIBCO/BRL)

This paper results from the Arthur M. Sackler Colloquium of the National Academy of Sciences, ''Regenerative Medicine,'' held October 18–22, 2002, at the Arnold and Mabel Beckman Center of the National Academies of Science and Engineering in Irvine, CA.

Abbreviations: DDC, 3,5-diethoxycarbonyl-1,4-dihydrocollidine; FACS, fluorescence-activated cell sorter; FAH, fumarylacetoacetate hydrolase; NTBC, 2-(2-nitro-4-trifluoromethylbenzoyl)-1,3-cyclohexanedione.

¶To whom correspondence should be addressed at: Department of Molecular and Medical Genetics, Oregon Health Sciences University, 3181 Southwest Sam Jackson Park Road, L103, Portland, OR 97239. E-mail: grompem@ohsu.edu.

containing 10% FBS, the cell suspension was left in a vertically positioned tube for 20 min on ice to let large hepatocytes sediment by gravity ($1 \times g$ for 20 min). The cells in the supernatant were then pelleted by spin for 5 min at 1,600 rpm ($\approx 400 \times g$) in a Sorvall RT7 centrifuge (DuPont).

We adapted the discontinuous Nycodenz (D-2158, Sigma) gradient described for the isolation of rat oval cells (25). Two kinds of Nycodenz stock solution at 30% (wt/vol) were prepared, either in Earle's basic salt solution (EBSS, GIBCO) with color (no. 24010-068, with phenol red) or in EBSS without color (no. 24015, clear). The stock solutions were then serially diluted to 26% (red), 19%, 15% (red), and 13% by using EBSS and sequentially layered in a sterile Ultra-Clear centrifuge tube (Beckman, no. 344059). Then, the pellet of nonparenchymal cells was resuspended in Nycodenz solution of 11% and loaded at the top of the gradient. Centrifugation was set at 8,000 rpm ($\approx 8{,}000 \times g$) for 30 min in a Beckman L5-50 Ultracentrifuge with a SW41 Ti swinging rotor, slow acceleration, and without brake. After centrifugation, cells were found at the four gradient interphases. The cells at each interphase were named F1, F2, F3, and F4, starting with F1 (11%/13% interphase) at the top. A 16 gauge needle was used to collect the cells in each layer by penetrating the wall of the transparent centrifugation tube. Cells were washed twice with DMEM containing 10% FBS.

For size profile determination, the fractions were analyzed with a Coulter Multisizer II. Data were analyzed by using MULTISIZER ACCUCOMP 1.19 software.

Immunostaining of F2 Cells. F2 cells (2×10^4) were centrifuged onto a glass slide at 500 rpm ($\approx 28 \times g$) for 5 min by using a Shandon Cytospin centrifuge. For CK19 and albumin staining, the cells were immediately fixed in cold acetone (-20°C) for 5 min, followed by air-drying for 20 min and incubation with PBS. Cells were then stained for 1 h with a rabbit polyclonal antibody anti-mouse albumin (Accurate Chemical & Scientific, Westbury, NY) at a 1:500 dilution mixed with a mouse monoclonal anti-CK19 antibody (ICN/Cappel Aurora, OH) at a dilution of 1:100. After washing, anti-mouse phycoerythrin (PE) and anti-rabbit FITC (Caltag, South San Francisco, CA) at a dilution of 1:100 each were used as secondary antibodies.

Fluorescence-Activated Cell Sorter (FACS) Analysis. Nonparenchymal cells were suspended at 1×10^7 per ml in PBS with 2% bovine serum. The cells were incubated with antibody at a 1:200 dilution for 40 min at 4°C, washed twice with staining buffer, and resuspended at 1×10^7 per ml for FACS sorting. Data were acquired by using a FACSVantage flow cytometer (BD Biosciences). The antibodies used for this experiment were FITC-conjugated anti-CD45.2 mAb (BD Biosciences, clone 104) and PE-conjugated anti-CD117 mAb (c-Kit, BD Biosciences, clone 2B8).

Cell Transplantation. Donor cells were resuspended in 100 μl of DMEM with 10% FBS and injected intrasplenically into *Fah*Δ^{exon5} recipient animals as described (32). All *Fah* mutant mice were kept on NTBC until the time of transplantation, when it was discontinued.

Histology and Immune Histology. Fah and CK19 immunohistochemistry were done as described (33). CK19 antibody was a generous gift from Lucie Germain (Laval University, Quebec City, QC, Canada), and the A6 antibody was a generous gift from Valentina Factor (National Cancer Institute, National Institutes of Health, Bethesda). Sections of paraformaldehyde-fixed tissue were deparaffinized and treated with periodic acid and sodium hydroboride to block endogenous peroxidase before staining with rat monoclonal antibody at 1:10 dilution for 30 min at room temperature. After rinsing, rabbit anti-rat antibody labeled with horseradish peroxidase was applied at 1:100 for 30 min at room temperature. Color was obtained with a Vector Laboratories ABC kit and diaminobenzidine/nickel chloride. For β-galactosidase whole-mount staining, liver tissues were fixed in 2% formaldehyde and 0.2% glutaraldehyde and incubated at 37°C overnight as described (34).

Southern Blot. Liver genomic DNA was isolated from random $5 \times 5 \times 5$-mm sections of tissue from the left main lobe (35). Genomic DNAs were digested with *Bam*HI (Pharmacia) and separated by 0.8% agarose gel. Capillary transfer and hybridization were performed according to standard protocols (36). For detection of the neomycin phosphotransferase gene used in generating the transgenic animals, the digested DNA blot was probed with a 680-bp *Pst*I (Pharmacia) fragment isolated from a neomycin phosphotransferase cDNA (32).

Semiquantitative PCR. To determine the ratio of wild-type and *Fah* mutant alleles in genomic DNA a three-primer competitive PCR was used (27). To quantitate the relative ratios of *Fah* to wild-type, the PCR products were hybridized with a ^{32}P-labeled oligonucleotide probe (5′-GGCATTATGTTCAGAGGC-3′) common to both PCR products. The intensities of both *Fah* mutant and wild-type signals were quantitated by using a Beckman SI Phosphoimager and compared with a standard curve generated by mixing known ratios of DNA from wild-type, *Fah* mutant ($-/-$), and *Fah* heterozygous ($+/-$) mice.

Semiquantitative PCR with four primers for *Rosa26* and wild-type alleles was performed under similar conditions as the *Fah* PCR. The forward (5′-GGTAACAGTTTCTTTATGGCAGGG-3′) and reverse primers (5′-ACCACCGCACGATAGAGATTCG-3′) produced a 175-bp band for *Rosa*26 DNA (29). The wild-type band, generated by forward primer 5′-GGCTTAAAGGCTAACCTGATGTG-3′ and reverse primer 5′-GCGAAGAGTTTGTCCTCAACC-3′, was 375 bp.

Results

Characterization of DDC-Treated Liver. Mice of the 129S$_4$ strain were put on a diet containing 0.1% DDC (wt/wt) as previously reported, and its effects were similar to those in C57/BL6 mice (26). The oval cell reaction peaked 3–4 weeks after initiation of the DDC treatment with an increase in liver weight by a factor of 1.5–2 (data not shown). Histological examination demonstrated both necrosis and apoptosis in hepatocytes (data not shown). In the periportal area a population of small cells emerged beginning on day 5 of treatment, spreading out in the liver lobule with time (Fig. 1). Proliferation of both hepatocytes and bile ducts were observed by BrdUrd labeling (Fig. 1*B*). Many of the small cells had duct-like morphology and with high level of proliferation (Fig. 1 *E* and *F*). However, cell division was not limited to the periportal cells because hepatocytes throughout the hepatic lobule continued to be labeled by BrdUrd during the entire process of DDC treatment (as long as 5 months). This suggests that DDC does not completely block hepatocyte proliferation, but rather induces a chronic regenerative state in the liver. Several antibodies were used to determine the properties of cells involved in the oval cell/atypical duct proliferation. The mouse hepatic oval cell marker A6 (37) was positive not only in the periportal oval cells (Fig. 1*C*) but also in some adjacent hepatocytes (Fig. 1*D*). Some of the small proliferating cells stained positive for the bile duct epithelial cell marker CK19 (Fig. 1 *E* and *F*), but all of these cells were negative for mature hepatocyte marker Fah (Fig. 1 *G* and *H*). Therefore, there were some small cells at the periportal region induced by DDC treatment that did not stain with either CK19 or Fah. This undefined population could represent either hematopoietic cells (inflammatory cells) or oval cell precursors.

Overall, the DDC diet induced the proliferation of hepato-

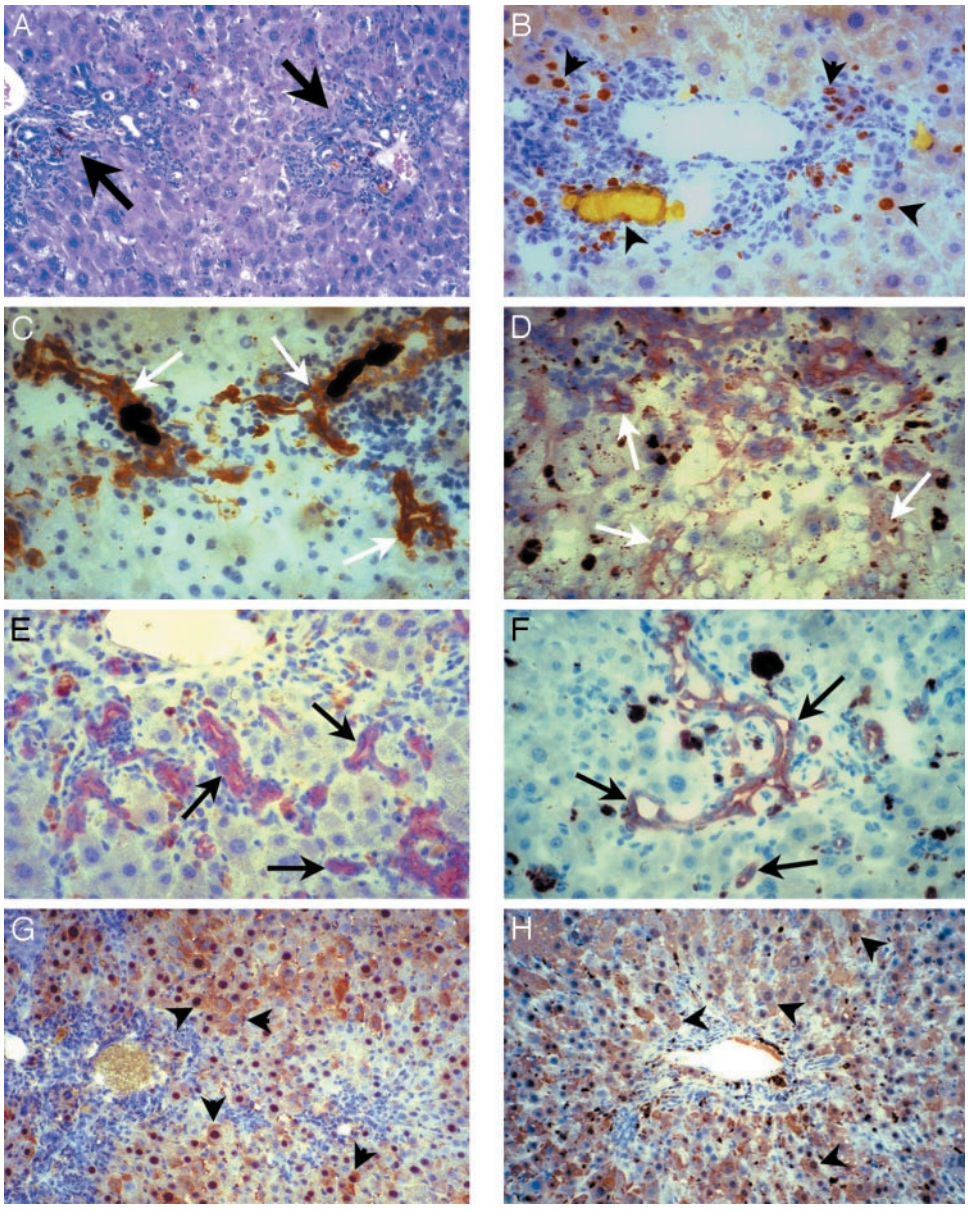

Fig. 1. Histology of DDC-treated liver. (*A*) Hematoxylin/eosin sample after 3 weeks. Arrows indicate the proliferating cells in the portal area. (*B*) BrdUrd staining (arrowheads) after 2 weeks of DDC treatment. (*C* and *D*) A6 antibody immunostaining (brown, arrows) at 3 (*C*) and 12 (*D*) weeks. A6 expression is seen in periportal small cells as well as some hepatocytes. (*E* and *F*) CK19 staining (arrows) at 3 (*E*) and 20 (*F*) weeks showing expansion of atypical duct cells. (*G* and *H*) Fah staining (arrowheads) at 3 (*G*) and 12 (*H*) weeks. The small periportal cells are Fah-negative.

cytes as well as small proliferating cells at the periportal region with duct morphology. The finding in the DDC model therefore differs from the typical models for oval cell proliferation in the rat (8, 38) and mouse (39), in which hepatocytes do not divide and where duct proliferation is less prominent.

Enrichment and Characterization of Oval Cells. To further characterize the DDC-induced oval cells/atypical duct cells, we enriched them on a discontinuous Nycodenz density gradient (25). Nonparenchymal liver cells were isolated from mice after DDC treatment for 3–4 weeks and from controls. Compared with control liver, the total number of nonparenchymal cells isolated from the DDC-treated liver was four to five times higher. The size profiles of nonparenchymal cells were analyzed (Fig. 2 *A* and *B*), and the DDC-treated livers showed a remarkable increase for cells in the F2 and F3 fractions compared with untreated controls (Fig. 2*C*). Previous reports on rat oval cells indicated that the size of rat oval cells was 8–10 μm in diameter and that they are found in the F2 fraction (25). In DDC-treated mice, the F1 and F2 fractions contained small cells with of 7–10 μm in diameter (Fig. 2*C*), similar to rat oval cells. Although the cell size in both F1 and F2 was similar, many more cells were present in the F2 fraction. The F3 fraction contained a mix of both small cells (7–10 μm) and larger cells (15–25 μm). F4 contained only large cells (15–25 μm). The large cells in the F3 and F4 fractions were hepatocytes, because many of them were binucleated (data not shown). The size profile of the F2 fraction suggested that it contained the majority of nonhepatocytes induced by DDC (Fig. 2*C*).

The Nycodenz-enriched F2 oval cell fraction was characterized by immunocytochemistry for albumin and CK19. Significant numbers of F2 cells had detectable albumin ($\approx$40%, Fig. 3*A*) or

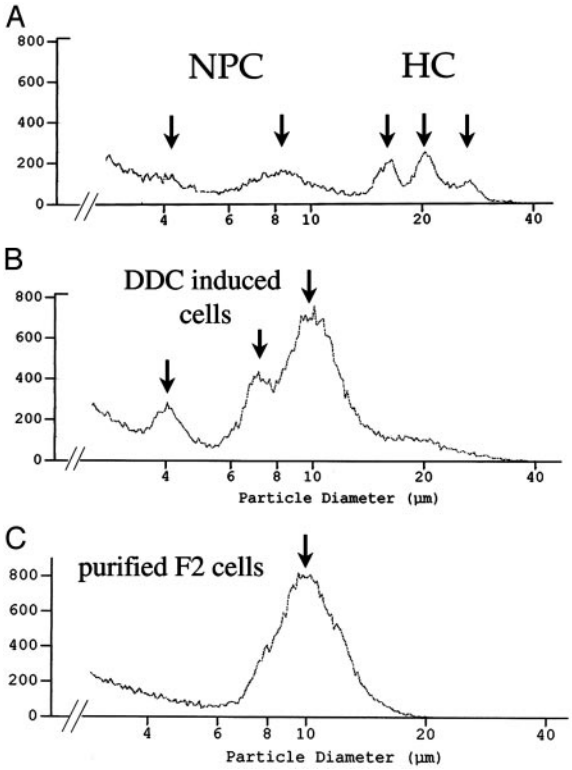

Fig. 2. Size profile of nonparenchymal cell fractions. (*A*) Normal liver. The peaks correspond to nonparenchymal cells (NPC) and hepatocytes (HC). (*B*) Liver after 3 weeks of DDC. There are three populations induced by DDC, which were the cells with diameters of 4, 7, and 10 μm. (*C*) F2 cell fraction of DDC-treated liver, consisting mostly of 10-μm cells.

CK-19 expression (40%, Fig. 3*B*). Interestingly, most of these cells were doubly stained for both albumin and CK-19 (Fig. 3*C*), similar to previous reports on rat oval cells (25). FACS analysis

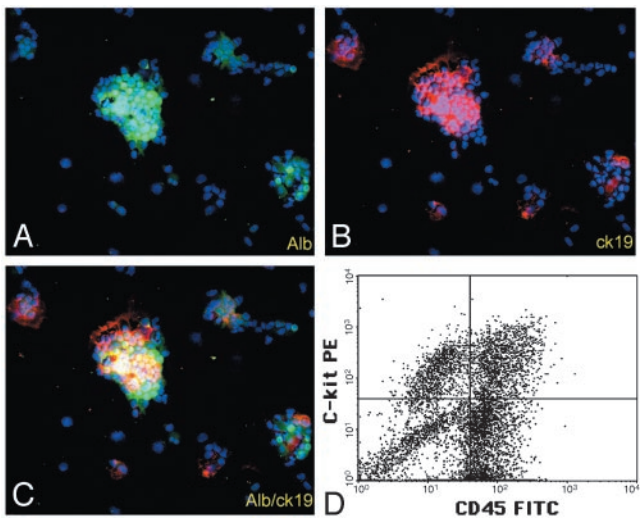

Fig. 3. Charazterization of the F2 cell fraction. F2 cells isolated by Nycodenz gradient centrifugation. (*A–C*) Immunocytochemistry of the same field. Blue stain is 4′,6-diamidino-2-phenylindole (DAPI) for nuclei. (*A*) albumin. (*B*) CK19. (*C*) albumin–CK19 overlay. (*D*) FACS analysis using antibodies to c-kit and CD45. About half (55%) of the cells were CD45-positive (hematopoietic in origin). The CD45-negative population could be divided into c-kit-positive and -negative cells.

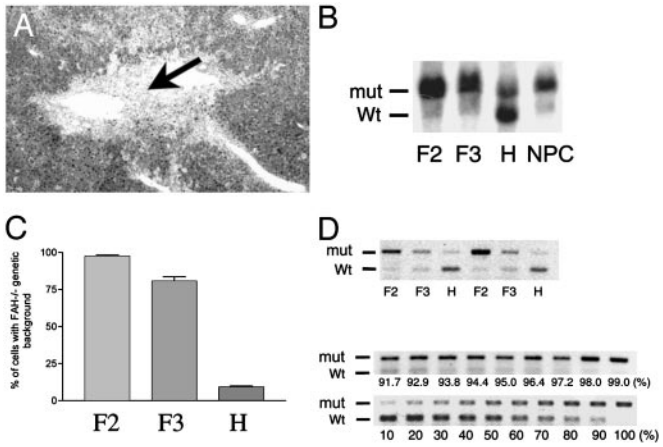

Fig. 4. Analysis of oval cells in chimeric livers. (*A*) Fah immunohistochemistry of a DDC-treated chimeric liver. Hepatocytes are stained dark (Fah-positive), whereas the periportal oval cells (arrow) are Fah-negative. (*B*) Southern blot using a probe to detect the *Fah* mutant (mut) and wild-type (Wt) alleles. DNA from the F2 and F3 Nycodenz cell fractions, hepatocytes (H), and unfractionated nonparenchymal cells (NPC) was analyzed. The nonparenchymal cells are predominantly Fah mutants, whereas hepatocytes are *Fah* wild-type. (*C*) Phosphoimager quantitation of Southern blot results shown in *D*. F2 = 97%, F3 = 81%, and H = 9% *Fah* mutant allele. (*D*) Semiquantitative PCR for the *Fah* genotypes. (*Upper*) Results from independently isolated F2 and F3 cells and hepatocytes (H). (*Lower*) Quantitation standards. F2 DNA contains >97% of the *Fah* mutant allele.

of the F2 cells was also performed by using c-kit and CD45 antibodies. About half of the F2 cell fraction was CD45 positive, indicating heavy contamination with hematopoietic cells. A subpopulation of c-kit-positive but CD45-negative cells (≈20%) could be detected and sorted by FACS (Fig. 3*D*). In the rat, c-kit is an oval cell marker (40), making this the most likely population to represent highly enriched oval cells. Overall, the data indicate that the F2 fraction of DDC-treated mouse liver is significantly enriched for oval cells (20–40%), but is also contaminated with hematopoietic cells (50–60%).

Do Oval Cells Arise by Dedifferentiation of Mature Hepatocytes? Next, we asked whether the oval/atypical duct cells observed in DDC-treated animals were of hepatocellular origin *in vivo*. To determine whether oval cells originated from hepatocytes, animals with chimeric livers were generated, in which the hepatocytes and nonparenchymal cells were genetically distinct. *Fah*−/− mice were transplanted with wild-type hepatocytes to produce chimeric livers in which >90% of the hepatocytes were donor-derived, i.e., *Fah*+/+ (Fig. 4*A*). After completed liver repopulation, NTBC was restarted to normalize hepatocyte function in the remaining *Fah*−/− cells. After 4 weeks of NTBC and normalization of body weight, the mice with chimeric livers were treated with a DDC diet for 3–6 weeks to induce oval cell proliferation. The mice were killed, and the oval cells were enriched by Nycodenz gradient. Their origin was determined by the their genotype. Both Southern blot and semiquantitative PCR were used (Fig. 4 *B* and *D*). In multiple independent experiments, ≥97% or more of the F2 fraction oval cells were of the *Fah*−/− (recipient) genotype (Fig. 4*C*). In contrast, ≥90% of the large cells (hepatocytes) were *Fah*+/+, as expected.

Because the absolute number of cells in the nonparenchymal fraction had increased at least 5-fold during DDC treatment, it can be concluded that most or all of the newly appearing oval cells were of host origin and not derived from dedifferentiating hepatocytes. This observation is consistent with previous reports

Table 1. Comparison of liver repopulation by different F2 cells

Source of F2 cells	Mice transplanted	Mice with Fah+ cells at 4 weeks	Dead during selection	Mice with Fah+ cells at 8 weeks	Mice with repopulation
Untreated mice	8	0/4	4/4	0/0	0
DDC-treated mice	10	1/4	2/6	4/4	5

based on the histological characterization of oval cell reactions (12, 15, 26).

Therapeutic Liver Reconstitution by Oval Cells. The results described above confirmed the nonparenchymal origin of oval cells. However, the ability of these cells to become functional hepatocytes remained unknown. Furthermore, the actual liver repopulation potential of oval cells (= non-hepatocyte-derived progenitors) has never been assessed in any model. Therefore, to determine whether DDC-induced oval cells were useful for therapeutic liver repopulation, purified cells of the F2 fraction were transplanted into *Fah*−/− recipients. Male *Rosa-26* mice (29) wild-type for *Fah* gene and transgenic for the *Escherichia coli* lacZ gene were used as donors. They were treated with the DDC diet for 3–4 weeks, and oval cells were enriched by Nycodenz gradient centrifugation for subsequent transplantation.

In the first experiment, purified oval cells of the F2 fraction from DDC-treated mice were compared with the same fraction isolated from a nontreated normal liver. In each case, 5×10^5 viable cells were transplanted intrasplenically and NTBC was stopped. About half of the total animals were killed and analyzed early (4 weeks after transplantation), whereas the others were subjected to prolonged NTBC withdrawal to determine whether they would be rescued by the transplantation. In the group transplanted with F2 cells from DDC-treated livers, four of six *Fah*−/− mutants subjected to long-term NTBC withdrawal had significant donor-derived hepatocyte repopulation and phenotypic rescue (Table 1 and Fig. 5*B*). In addition, one of four mice harvested early had readily detectable donor-derived nodules. In contrast, four of four recipients of F2 fraction cells from normal liver had no detectable donor cell-derived repopulation at the early harvest (Table 1) and none survived past 6 weeks. This result suggested that DDC-induced oval cells were able to differentiate into fully functional hepatocytes and repopulate the *Fah*−/− liver. On the other hand, similar sized nonparenchymal cells from untreated normal liver were not capable of liver repopulation. Therefore, DDC-induced oval cells functioned as transplantable hepatocyte progenitors.

The oval cell enrichment used here provides an enriched but not completely pure population (Figs. 2*C* and 3). Therefore, the possibility existed that contaminating hepatocytes could be responsible for the observed liver repopulation. To prove definitively that contaminating hepatocytes were not responsible for liver repopulation by the F2 cell fraction, competitive repopulation experiments were performed. Multiple experiments had indicated that the level of hepatocyte contamination was ≤2% (Fig. 2*C*). Therefore, oval cells isolated from *Rosa-26* mice were cotransplanted with 2% hepatocytes from mice heterozygous for a mutation in the Fanconi anemia group C gene (*Fancc*). All mice used were congenic on the $129S_4$ strain. The hepatocytes from the DDC-treated *Fancc* heterozygotes were treated with the identical cell digestion and isolation protocol as the DDC-induced oval cells. A total of 150,000 oval cells were cotransplanted intrasplenically with 3,000 hepatocytes into *Fah* mutant mice. After 6–8 weeks, DNA from repopulated livers was analyzed by Southern blot using a probe that produced distinct restriction fragments in *Fah*−/−, *Fancc*+/−, and *Rosa-26* mice. Repopulated livers displayed no measurable contribution of the *Fancc* genotype of the hepatocytes, whereas the *Rosa-26* oval cell genotype was readily observed (Fig. 5*A*). To further address the issue of possible hepatocyte contamination, hepatocytes and oval cells were also competed at a 1:1 ratio. In this case, the oval cells and hepatocytes contributed equally to repopulation (Fig. 5*A*). It should be noted that the competing hepatocytes were from DDC-treated mice and that they had been isolated with the severe protease digestion protocol used for oval cells. Therefore, the competition experiments did not compare the repopulation potential of optimally isolated hepatocytes with that of oval cells.

Additionally, several *Fah*−/− mice were transplanted with c-kit-positive/CD45-negative F2 fraction cells isolated by FACS from DDC-treated *Rosa-26* donors. Significant liver repopulation was detectable by whole-mount β-galactosidase staining (Fig. 6*A*), suggesting that this specific population of oval cells has liver repopulating activity.

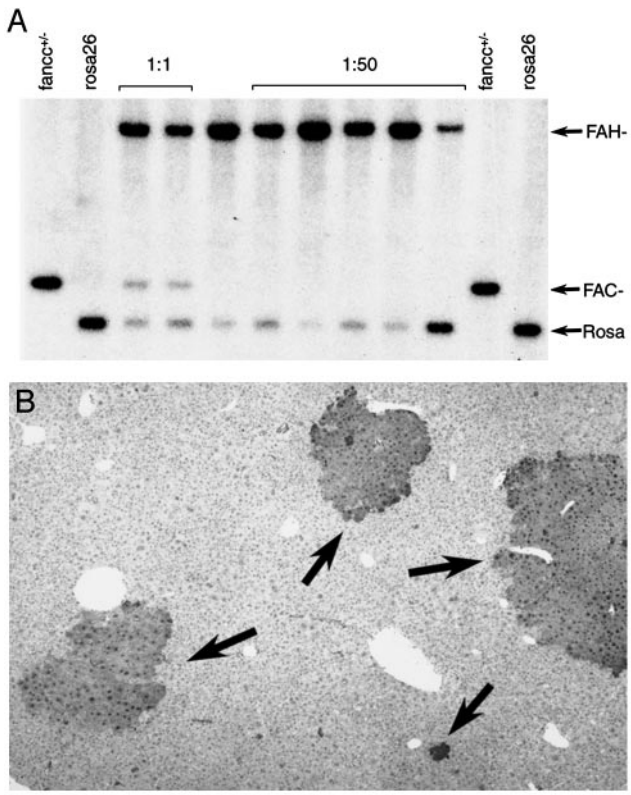

Fig. 5. Liver repopulation by oval cells. (*A*) Competitive repopulation experiments. DNA from repopulated liver was probed with a neomycin-resistance gene fragment that detects different-sized fragments for the *Fancc*+/−, *Rosa26*+/−, and *Fah*−/− mutant strains of mice. Control DNA from the donor strains is shown in the two outermost lanes on each side. In the lanes marked 1:1, equal numbers of *Fancc*+/− hepatocytes and *Rosa26*+/− F2 fraction oval cells were cotransplanted. In the lanes marked 1:50, the ratio of hepatocytes to oval cells was 1:50. Hepatocytes and F2 cells contributed equally to repopulation when competed 1:1. All detectable repopulation was effected by the oval cells at the 1:50 ratio. (*B*) Fah immunohistochemistry shows oval cell-derived Fah+ hepatocyte nodules (arrows) in mutant liver after 8 weeks of transplantation.

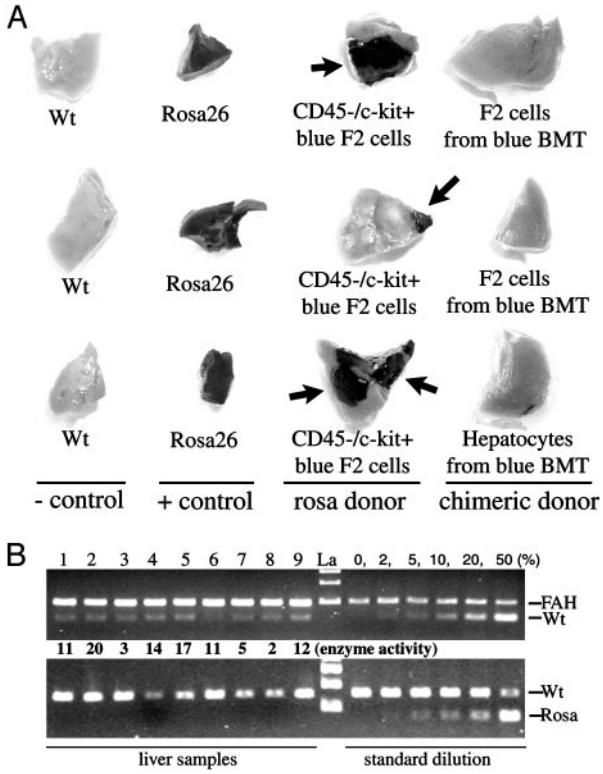

Fig. 6. Liver repopulation by oval cells from bone marrow chimeras. (*A*) Whole-mount β-galactosidase staining of liver from secondary recipients transplanted with liver cells from mice whose hematopoietic system had been replaced by lacZ-expressing cells (*Rosa26*+/−). The donor mice had been treated with DDC for 7 months. Controls for staining included wild-type (Wt) and *Rosa-26* livers in the two left lanes. Controls for the transplantation included mice transplanted with CD45−/c-kit+ oval cells from a DDC-treated *Rosa26*+/− mouse (third lane from left). Dark staining (arrows) indicates areas of repopulation by lacZ-expressing hepatocytes. No blue staining was detectable in any secondary recipients of bone marrow chimeric mice, regardless of whether the donor cells were F2 cells or hepatocytes (far right lane). This result indicates that the oval cells and hepatocytes of the donor animals did not originate in the hematopoietic system. (*B*) Semiquantitative PCR of liver DNA aliquots from nine secondary recipients. Lanes 1–4 were from oval cell recipients, and lanes 5–9 were from hepatocyte recipients. The percentage of the *Fah* wild-type allele was 10–30% in all samples, whereas the *Rosa-26* allele was not detectable in the same samples. The corresponding Fah enzyme activity measured is shown below each lane of Fah PCR (given in % of wild-type activity). Therefore, all observable liver repopulation was due to nonhematopoietic cells.

Together, these experiments showed that differentiated hepatocytes are not the only cell type capable of liver reconstitution and that murine oval cells were capable of significant therapeutic liver repopulation.

Do Oval Cells Come from the Bone Marrow? The results obtained with transplantation of oval cells were consistent with a nonhepatocyte source for tissue repair in liver injury. Previous work had demonstrated that oval cells in the rat could be bone marrow-derived (17). In addition, oval cells have been shown to share cell surface markers such as Thy-1 and c-kit with hematopoietic cells (40, 41). We therefore wished to determine whether the DDC-induced oval cells originated from the bone marrow. Toward this end, bone marrow transplantation was carried out in wild-type mice of the $129S_4$ strain by using congenic *Rosa-26* mice as donors. Lethally irradiated hosts were given 2×10^6 bone marrow cells and achieved >95% hematopoietic engraftment (data not shown). After >3 months, the transplanted animals were started on a DDC diet to induce oval cell proliferation. To maximize the potential of bone marrow cells to repopulate the oval cell compartment, mice were exposed to DDC continuously for as long as 7 months. After 7 months, three independent animals were killed. Hepatocytes and oval cells (F2 fraction) were isolated from each liver and serially transplanted into at least three nonirradiated *Fah* mutant secondary recipients each. Genotyping showed that the F2 oval cell fraction contained ≈50% cells of the bone marrow genotype (*Rosa-26*). This was not surprising, because FACS analysis had shown previously that approximately half of the F2 cells were positive for the hematopoietic cell-surface marker CD45 (Fig. 2*D*). The hepatocyte fraction, however, was predominantly negative for *Rosa-26* (data not shown), indicating that the bone marrow had not significantly contributed to this fraction despite months of hepatocyte turnover.

After 8–12 weeks of selection, the degree of liver repopulation in secondary transplant recipients and the genotype of the liver repopulating cells were determined by quantitative genotyping and also measurement of the Fah enzyme activity. As expected, Fah+ liver population ranging from 10% to 30% was found in all secondary recipients (Fig. 6). Importantly, the genotype analysis showed that >99% of the liver repopulating cells were *Rosa-26*-negative and therefore not derived from the original bone marrow. This conclusion was also verified by whole-mount β-galactosidase staining of the repopulated livers (Fig. 6*A*). No blue staining was observed in the repopulated secondary recipient livers, whereas controls transplanted with F2 cells from DDC-treated *Rosa-26* mice clearly displayed blue nodules (Fig. 6*A*). Overall, these data show that bone marrow-derived cells did not contribute significantly to the oval cell or hepatocyte populations of DDC-treated mice even after several months of chronic liver injury.

Discussion

Oval Cells Are Derived from Intrahepatic Precursors. The origin of hepatic oval cells has been studied for the last 20 years (11). Many early reports suggested that oval cells came from the bile ducts of the portal region. More recent studies in 2-acetylaminofluorene-treated rats have pinpointed the origin of oval cells to be the terminal bile ductules (also named the Canals of Hering) that are the junctions between bile duct epithelial cells and hepatocytes (12). However, these findings did not rule out the possibility that oval cells could also be derived from other cells in the liver. *In vitro* studies have shown that mature hepatocytes can convert to a bile duct phenotype (20, 21). This has given rise to the hypothesis that there is no lineage hierarchy in the oval cell reaction (18, 42). Similarly, experiments using chimeric livers have shown that primitive liver cell phenotypes induced by carcinogens can be derived from mature hepatocytes (19). Others have suggested recently that oval cells and hepatocytes have an extrahepatic origin and are derived from the bone marrow and not the liver itself (17, 41, 43–46). It has also been proposed that extrahepatic stem cells may represent a significant source for tissue repair in liver injury (47, 48). According to this model, hepatocyte replacement by bone marrow-derived progenitors could occur either directly by stem cells differentiating into hepatocytes or indirectly via an oval cell intermediate.

Here, we addressed these hypotheses in a well characterized model of chronic liver injury and oval cell proliferation in the mouse. The experiments showed that the oval cells induced by chronic administration of DDC neither derived from mature hepatocytes nor originated in significant proportions from progenitors in the bone marrow. Thus, our observations were most consistent with the classic model where preexisting intrahepatic stem cells/progenitors residing in the portal region are induced to become oval cells that then differentiate into hepatocytes. Our working model is summarized in Fig. 7. The liver-resident stem

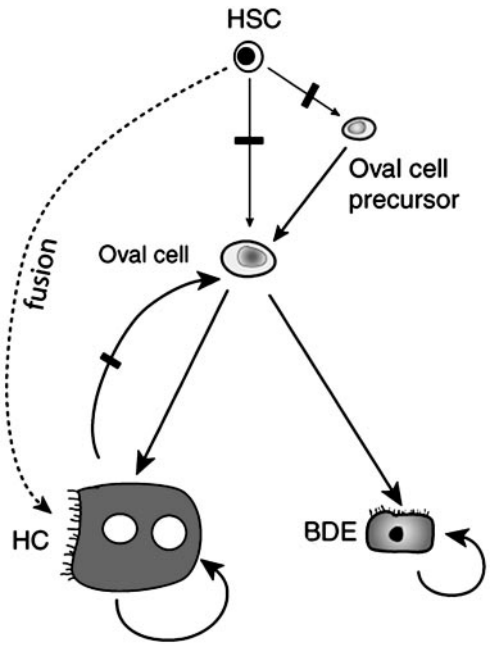

Fig. 7. Model for liver stem cell hierarchy. In a chronic injury setting intrahepatic oval cell precursors produce oval cells, which can differentiate into either hepatocytes (HC) or bile duct epithelium (BDE). The reverse, i.e., dedifferentiation of hepatocytes to oval cells, does not occur. Hematopoietic stem cells (HSC) do not serve as precursors for oval cells, either directly or indirectly. Bone marrow-derived hepatocytes originate by cell fusion.

cells were not replaced from the bone marrow, even during 7 months of liver injury, representing one-third of the lifetime of a mouse. These results are consistent with previous findings that bone marrow-derived hepatocytes are too rare and appear too slowly to effect efficient injury repair in a semiacute setting (33, 49, 50). Furthermore, we have recently shown that bone marrow-derived hepatocytes are generated by *in vivo* cell fusion, not stem cell differentiation (51).

It should be noted, however, that our findings cannot be generalized at this time. We used liver repopulating ability to functionally define oval cells as hepatocyte progenitors, whereas others have used morphological criteria (10, 41). Thus, our findings may apply narrowly only to liver repopulating oval cells. In addition, the oval cell response in DDC-treated mice differs from the classic rat models because hepatocytes can still divide, whereas most oval cell regimens in the rat block hepatocyte proliferation (3). The work presented here shows that oval cells can be generated without bone marrow progenitors in at least some settings. It is formally possible that other forms of liver damage could result in significant contribution of bone marrow progenitors to liver regeneration.

Oval Cells Can Repopulate the Liver. Earlier studies have shown that rat oval cells are capable of differentiating into cells expressing multiple hepatocyte-specific markers *in vitro* (10, 52, 53). Similarly, primary pancreatic oval cells (25) and an immortal oval cell line (54) can differentiate into hepatocyte-like cells on transplantation into the liver *in vivo*. Surprisingly, however, no reports on liver repopulation by oval cells or functional rescue of a liver disease by oval cell transplantation have been reported (55). It was therefore unclear whether the reported differentiation of adult oval cells into "hepatocytes" was functionally relevant and whether oval cells could serve as a source of transplantable, therapeutically effective hepatocyte precursors. The results shown here indicate that DDC-induced murine oval cells were indeed capable of liver repopulation and could rescue a metabolic liver disease. To our knowledge, this is the first demonstration of the therapeutic efficiency of liver resident nonhepatocytes derived from adult liver. Nonetheless, the repopulation by oval cells was considerably slower and less complete than expected for the equivalent number of hepatocytes (33). There are a couple of potential reasons for this. First, the cells of F2 fraction transplanted here were heavily contaminated by hematopoietic cells and possibly other non-oval cell types. Second, engraftment of oval cells may be less efficient than for hepatoctyes because of their smaller size and less efficient trapping in the liver. To determine the true therapeutic potential of oval cells, it will be necessary to purify them to homogeneity in the future and to measure their rate of initial liver engraftment.

Overall, the results described here provide encouragement for the development of intrahepatic progenitors in transplantation. These cells have several potential advantages over regular hepatocytes. First, oval cells can be expanded in culture (24, 56), which is very difficult to do for primary hepatocytes. Second, oval cells are "hardier" and more resistant to protease digestion than primary hepatocytes. It may therefore be possible to isolate these cells from cadaveric donor livers or other specimens that are unsuitable for orthotopic transplantation or isolation of viable hepatocytes. Finally, oval cells are multipotential and may have therapeutic benefit in diseases of the biliary tree (10) or possibly even the pancreas (57).

We thank Angela Major and Billie Smith for their support with histological analysis. This work was supported by National Institutes of Health Grant RO1-DK48252 (to M.G.) and the Juvenile Diabetes Foundation (X.W.).

1. Michalopoulos, G. K. & DeFrances, M. C. (1997) *Science* **276,** 60–66.
2. Grompe, M. & Finegold, M. (2001) in *Stem Cell Biology*, eds. Marshak, D. R., Gardner, R. L. & Gottlieb, D. (Cold Spring Harbor Lab. Press, Plainview, NY), pp. 455–497.
3. Fausto, N. & Campbell, J. S. (2003) *Mech. Dev.* **120,** 117–130.
4. Shinozuka, H., Lombardi, B., Sell, S. & Iammarino, R. M. (1978) *Cancer Res.* **38,** 1092–1098.
5. Solt, D. B., Medline, A. & Farber, E. (1977) *Am. J. Pathol.* **88,** 595–618.
6. Potten, C. S. (1997) *Stem Cells* (Academic, London).
7. Thorgeirsson, S. S. (1996) *FASEB J.* **10,** 1249–1256.
8. Alison, M., Golding, M., Lalani, E. N., Nagy, P., Thorgeirsson, S. & Sarraf, C. (1997) *J. Hepatol.* **26,** 343–352.
9. Fausto, N. (1994) in *The Liver: Biology and Pathobiology*, ed. Arias, I. M. (Raven, New York), pp. 1501–1518.
10. Lemire, J. M., Shiojiri, N. & Fausto, N. (1991) *Am. J. Pathol.* **139,** 535–552.
11. Sell, S. & Ilic, Z. (1997) *Liver Stem Cells* (Landes, Austin, TX/Chapman & Hall, New York).
12. Paku, S., Schnur, J., Nagy, P. & Thorgeirsson, S. S. (2001) *Am. J. Pathol.* **158,** 1313–1323.
13. Plenat, F., Braun, L. & Fausto, N. (1990) *Zentralbl. Allg. Pathol.* **136,** 135–149.
14. Golding, M., Sarraf, C. E., Lalani, E. N., Anilkumar, T. V., Edwards, R. J., Nagy, P., Thorgeirsson, S. S. & Alison, M. R. (1996) *Gastroenterology* **110,** 1182–1190.
15. Novikoff, P. M., Ikeda, T., Hixson, D. C. & Yam, A. (1991) *Am. J. Pathol.* **139,** 1351–1368.
16. Theise, N. D., Saxena, R., Portmann, B. C., Thung, S. N., Yee, H., Chiriboga, L., Kumar, A. & Crawford, J. M. (1999) *Hepatology* **30,** 1425–1433.
17. Petersen, B. E., Bowen, W. C., Patrene, K. D., Mars, W. M., Sullivan, A. K., Murase, N., Boggs, S. S., Greenberger, J. S. & Goff, J. P. (1999) *Science* **284,** 1168–1170.
18. Block, G. D., Locker, J., Bowen, W. C., Petersen, B. E., Katyal, S., Strom, S. C., Riley, T., Howard, T. A. & Michalopoulos, G. K. (1996) *J. Cell Biol.* **132,** 1133–1149.
19. Braun, K. M. & Sandgren, E. P. (2000) *Am. J. Pathol.* **157,** 561–569.
20. Coleman, W. B. & Presnell, S. C. (1996) *Hepatology* **24,** 1542–1546.
21. Michalopoulos, G. K., Bowen, W. C., Mule, K., Lopez-Talavera, J. C. & Mars, W. (2002) *Hepatology* **36,** 278–283.
22. Grompe, M., Laconi, E. & Shafritz, D. A. (1999) *Semin. Liver Dis.* **19,** 7–14.

23. Shafritz, D. A., Dabeva, M. D. & Grompe, M. (2001) in *The Liver: Biology and Pathobiology*, ed. Arias, I. M. (Lippincott Williams & Wilkins, Philadelphia), pp. 927–940.
24. Sirica, A. E., Mathis, G. A., Sano, N. & Elmore, L. W. (1990) *Pathobiology* **58,** 44–64.
25. Dabeva, M. D., Hwang, S. G., Vasa, S. R., Hurston, E., Novikoff, P. M., Hixson, D. C., Gupta, S. & Shafritz, D. A. (1997) *Proc. Natl. Acad. Sci. USA* **94,** 7356–7361.
26. Preisegger, K. H., Factor, V. M., Fuchsbichler, A., Stumptner, C., Denk, H. & Thorgeirsson, S. S. (1999) *Lab. Invest.* **79,** 103–109.
27. Grompe, M., Al-Dhalimy, M., Finegold, M., Ou, C. N., Burlingame, T., Kennaway, N. G. & Soriano, P. (1993) *Genes Dev.* **7,** 2298–2307.
28. Overturf, K., Al-Dhalimy, M., Tanguay, R., Brantly, M., Ou, C. N., Finegold, M. & Grompe, M. (1996) *Nat. Genet.* **12,** 266–273.
29. Zambrowicz, B. P., Imamoto, A., Fiering, S., Herzenberg, L. A., Kerr, W. G. & Soriano, P. (1997) *Proc. Natl. Acad. Sci. USA* **94,** 3789–3794.
30. Lindstedt, S., Holme, E., Lock, E. A., Hjalmarson, O. & Strandvik, B. (1992) *Lancet* **340,** 813–817.
31. Grompe, M., Lindstedt, S., Al-Dhalimy, M., Kennaway, N. G., Papaconstantinou, J., Torres-Ramos, C. A., Ou, C. N. & Finegold, M. (1995) *Nat. Genet.* **10,** 453–460.
32. Overturf, K., Al-Dhalimy, M., Finegold, M. & Grompe, M. (1999) *Am. J. Pathol.* **155,** 2135–2143.
33. Wang, X., Montini, E., Al-Dhalimy, M., Lagasse, E., Finegold, M. & Grompe, M. (2002) *Am. J. Pathol.* **161,** 565–574.
34. MacGregor, G. R., Mogg, A. E., Burke, J. F. & Caskey, C. T. (1987) *Somatic Cell Mol. Genet.* **13,** 253–265.
35. Miller, S. A., Dykes, D. D. & Polesky, H. F. (1988) *Nucleic Acids Res.* **16,** 1215.
36. Sambrook, J., Fritsch, E. F. & Maniatis, T. (1989) *Molecular Cloning: A Laboratory Manual* (Cold Spring Harbor Lab. Press, Plainview, NY).
37. Faktor, V. M., Engel'gardt, N. V., Iazova, A. K., Lazareva, M. N., Poltoranina, V. S. & Rudinskaia, T. D. (1990) *Ontogenez* **21,** 625–632.
38. Alison, M. R., Golding, M., Sarraf, C. E., Edwards, R. J. & Lalani, E. N. (1996) *Gastroenterology* **110,** 1182–1190.
39. Factor, V. M., Radaeva, S. A. & Thorgeirsson, S. S. (1994) *Am. J. Pathol.* **145,** 409–422.
40. Fujio, K., Evarts, R. P., Hu, Z., Marsden, E. R. & Thorgeirsson, S. S. (1994) *Lab. Invest.* **70,** 511–516.
41. Petersen, B. E., Goff, J. P., Greenberger, J. S. & Michalopoulos, G. K. (1998) *Hepatology* **27,** 433–445.
42. Michalopoulos, G. K., Bowen, W. C., Zajac, V. F., Beer-Stolz, D., Watkins, S., Kostrubsky, V. & Strom, S. C. (1999) *Hepatology* **29,** 90–100.
43. Theise, N. D., Nimmakayalu, M., Gardner, R., Illei, P. B., Morgan, G., Teperman, L., Henegariu, O. & Krause, D. (2000) *Hepatology* **32,** 11–16.
44. Theise, N. D., Badve, S., Saxena, R., Henegariu, O., Sell, S., Crawford, J. M. & Krause, D. S. (2000) *Hepatology* **31,** 235–240.
45. Krause, D. S., Theise, N. D., Collector, M. I., Henegariu, O., Hwang, S., Gardner, R., Neutzel, S. & Sharkis, S. J. (2001) *Cell* **105,** 369–377.
46. Alison, M. R., Poulsom, R., Jeffery, R., Dhillon, A. P., Quaglia, A., Jacob, J., Novelli, M., Prentice, G., Williamson, J. & Wright, N. A. (2000) *Nature* **406,** 257.
47. Theise, N. D. & Krause, D. S. (2002) *Leukemia* **16,** 542–548.
48. Petersen, B. E. (2001) *Blood Cells Mol. Dis.* **27,** 590–600.
49. Mallet, V. O., Mitchell, C., Mezey, E., Fabre, M., Guidotti, J. E., Renia, L., Coulombel, L., Kahn, A. & Gilgenkrantz, H. (2002) *Hepatology* **35,** 799–804.
50. Mitchell, C. & Fausto, N. (2002) *Am. J. Pathol.* **161,** 349–350.
51. Wang, X., Willenbring, H., Akkari, Y., Tomimaru, Y., Foster, M., Al-Dhalimy, M., Lagasse, E., Finegold, M., Olson, S. & Grompe, M. (2003) *Nature*, in press.
52. Shiojiri, N., Lemire, J. M. & Fausto, N. (1991) *Cancer Res.* **51,** 2611–2620.
53. Fausto, N., Lemire, J. M. & Shiojiri, N. (1993) *Proc. Soc. Exp. Biol. Med.* **204,** 237–241.
54. Coleman, W. B., McCullough, K. D., Esch, G. L., Faris, R. A., Hixson, D. C., Smith, G. J. & Grisham, J. W. (1997) *Am. J. Pathol.* **151,** 353–359.
55. Laconi, E., Oren, R., Mukhopadhyay, D. K., Hurston, E., Laconi, S., Pani, P., Dabeva, M. D. & Shafritz, D. A. (1998) *Am. J. Pathol.* **153,** 319–329.
56. Germain, L., Noel, M., Gourdeau, H. & Marceau, N. (1988) *Cancer Res.* **48,** 368–378.
57. Yang, L., Li, S., Hatch, H., Ahrens, K., Cornelius, J. G., Petersen, B. E. & Peck, A. B. (2002) *Proc. Natl. Acad. Sci. USA* **99,** 8078–8083.